Brazilian Journal of Physics
ISSN: 0103-9733
luizno.bjp@gmail.com
Sociedade Brasileira de Física
Brasil

Kremer, Gilberto M.; Sobreiro, Octavio A. S.
Bulk Viscous Cosmological Model with Interacting Dark Fluids
Brazilian Journal of Physics, vol. 42, núm. 1-2, 2012, pp. 77-83
Sociedade Brasileira de Física
Sâo Paulo, Brasil

Braz J Phys (2012) 42:77–83
DOI 10.1007/s13538-011-0051-0

SOCIEDADE BRASILEIRA DE FÍSICA

PARTICLES AND FIELDS

Bulk Viscous Cosmological Model with Interacting Dark Fluids

Gilberto M. Kremer · Octavio A. S. Sobreiro

Received: 17 June 2011 / Published online: 18 November 2011

Abstract We study a cosmological model for a spatially flat Universe whose constituents are a dark energy field and a matter field comprising baryons and dark matter. The constituents are assumed to interact with each other, and a non-equilibrium pressure is introduced to account for irreversible processes. We take the non-equilibrium pressure to be proportional to the Hubble parameter within the framework of a first-order thermodynamic theory. The dark energy and matter fields are coupled by their barotropic indexes, which depend on the ratio between their energy densities. We adjust the free parameters of the model to optimize the fits to the Hubble parameter data. We compare the viscous model with the non-viscous one, and show that the irreversible processes cause the dark-energy and matter-density parameters to become equal and the decelerated–accelerated transition to occur at earlier times. Furthermore, the density and deceleration parameters and the distance modulus have the correct behavior, consistent with a viable scenario of the present status of the Universe.

Keywords Interacting dark fluids · Viscous cosmology

1 Introduction

The cosmic observations from the type Ia supernovae [1–4] suggest that the present period of the Universe is undergoing an accelerated expansion. Since matter contributes with attractive forces and positive pressure, which decelerate the expansion, an exotic component—the so-called dark energy—with negative pressure must be postulated to take into account the present accelerated expansion. Another dark component is necessary to explain the measured rotation curves of spiral galaxies [5]. This component, called dark matter, interacts only gravitationally with ordinary matter. Although dark energy can be modeled by a cosmological constant [6–10], the latter suffers from the so-called fine-tuning and cosmic coincidence problems [11–13]. Several models for the dark energy with dynamical properties have hence been analyzed in the literature. Among these, we mention scalar fields, tachyon fields, fermion fields, phantom fields, and exotic equations of state.

One expects the dark components not to evolve separately. Indeed, a promising resolution of the above-mentioned problems is known to stem from the assumption that the dark energy interacts with the dark matter. The interaction is assumed to be negligible at high red shifts, while it is preponderant at lower red shifts. This may also alleviate the coincidence problem, since an appropriate choice of the interaction term makes the ratio between the energy densities of the matter field and dark energy nearly constant at low red shifts. Several cosmological models have been proposed with interacting dark components; see [14–29] for examples. On the other hand, irreversible processes in the evolution of the Universe may also contribute significantly to alleviate the coincidence problem. In the Friedmann–Robertson–Walker metric, the source of irreversibility is a bulk viscosity associated with a non-equilibrium pressure (see, e.g., [30–40, 49, 50]).

G. M. Kremer (✉) · O. A. S. Sobreiro
Departamento de Física, Universidade Federal do Paraná,
Caixa Postal 19044, 81531-990 Curitiba,
Paraná, Brazil
e-mail: kremer@fisica.ufpr.br

This work proposes to develop a cosmological model for a spatially flat Universe with interacting dark components subject to irreversible processes. We follow [41] and couple the dark energy and matter fields by their barotropic indexes, which are functions of the ratio between their energy densities. This is in contrast with most of the literature, which considers an explicit form for the interaction term. In addition, in the framework of a first-order thermodynamic theory, we introduce a non-equilibrium pressure, which is responsible for the irreversible processes.

The paper is structured as follows: Section 2 discusses the general features of the proposed model for the Universe, with dissipative effects and interacting dark fluids. The analysis of the consequent cosmological constraints and cosmological solutions is the subject of Section 3. Finally, in Section 4, we present our conclusions.

2 Dissipative Interacting Dark Fluids

Let us consider a homogeneous, isotropic, and spatially flat Universe described by the Friedmann–Robertson–Walker metric $\mathrm{d}s^2 = \mathrm{d}t^2 - a(t)^2(\mathrm{d}x^2 + \mathrm{d}y^2 + \mathrm{d}z^2)$ where $a(t)$ denotes the cosmic scale factor. Furthermore, let us consider a cosmological model in which the Universe is a mixture of two constituents, namely dark energy (de) and matter (m) which represents the dark matter and baryons, respectively. In this model, a non-equilibrium pressure accounts for irreversible processes, and energy is assumed to be transferred between the dark energy and the matter field. The Friedmann equation and the evolution equation for the total energy density $\rho = \rho_\mathrm{m} + \rho_\mathrm{de}$ read

$$3H^2 = \rho_\mathrm{m} + \rho_\mathrm{de}, \tag{1}$$

$$\dot{\rho}_\mathrm{m} + \dot{\rho}_\mathrm{de} + 3H(\rho_\mathrm{m} + \rho_\mathrm{de} + p_\mathrm{m} + p_\mathrm{de} + \varpi) = 0. \tag{2}$$

In the above equations, $H = \dot{a}/a$ denotes the Hubble parameter, $p = p_\mathrm{m} + p_\mathrm{de}$ is the total equilibrium pressure, and ϖ stands for the non-equilibrium pressure, also known as the dynamic pressure.

We follow [41] and decouple (2) into two "effective conservation equations," namely

$$\dot{\rho}_\mathrm{m} + 3H\gamma^e_\mathrm{m}\rho_\mathrm{m} = 0, \tag{3a}$$

$$\dot{\rho}_\mathrm{de} + 3H\gamma^e_\mathrm{de}\rho_\mathrm{de} = 0. \tag{3b}$$

Here, the effective barotropic indexes γ^e_i $(i = \mathrm{m}, \mathrm{de})$ were introduced, which are related to each other by the equality

$$\gamma^e_\mathrm{m} = \gamma_\mathrm{m} + \frac{\gamma_\mathrm{de} - \gamma^e_\mathrm{de}}{r} + \frac{\varpi}{\rho_\mathrm{m}}, \tag{4}$$

where $r = \rho_\mathrm{m}/\rho_\mathrm{de}$ denotes the ratio between the energy densities, and the γ_i $(i = \mathrm{m}, \mathrm{de})$ represent constant barotropic indexes of the equations of state $p_i = (\gamma_i - 1)\rho_i$. We introduce this decoupling because we assume no explicit form for the interaction term between dark matter and dark energy. Rather, we consider this interaction to be intrinsically connected to the barotropic indexes.

Once again following [41], we assume the effective barotropic index of the dark energy to be given by

$$\gamma^e_\mathrm{de} = \gamma_\mathrm{de} - F(r), \tag{5}$$

where $F(r)$ is a function which depends only on the ratio of the energy densities r. The physical motivation for this choice is provided by the interaction between the dark fluids. Indeed, while γ^e_m and γ^e_de give the influence of the interaction term in the field equations, $F(r)$ accounts for the nature of this interaction. Since we are concerned with the coincidence problem, it is reasonable to assume F to depend on the ratio $r = \rho_\mathrm{m}/\rho_\mathrm{de}$. By taking into account the previous representation for γ^e_de, we can rewrite (3) as

$$\dot{\rho}_\mathrm{m} + 3H\gamma_\mathrm{m}\rho_\mathrm{m} = -3H\rho_\mathrm{de}F - 3H\varpi, \tag{6}$$

$$\dot{\rho}_\mathrm{de} + 3H\gamma_\mathrm{de}\rho_\mathrm{de} = 3H\rho_\mathrm{de}F. \tag{7}$$

Within the framework of ordinary (first order or Eckart) thermodynamic theory, the non-equilibrium pressure (see, e.g., [30–40]) is proportional to the Hubble parameter H, the proportionality factor being identified with the coefficient of bulk viscosity η, i.e., $\varpi = -3\eta H$. According to kinetic theory of relativistic gases (see, e.g., [42]), the bulk viscosity is proportional to the temperature with an exponent dependent on the intermolecular forces. It is therefore usual in cosmology to assume that $\eta \propto \rho^m$, where m is a positive constant.

Under the assumption that the coefficient of bulk viscosity is proportional to the square root of the total energy density—$\eta = \eta_0\sqrt{\rho}$ with η_0 a constant—the field equations are integrable, and the expression for the effective barotropic indexes (4) becomes

$$\gamma^e_\mathrm{m} = \gamma_\mathrm{m} + \frac{\gamma_\mathrm{de} - \gamma^e_\mathrm{de}}{r} - \sqrt{3}\left(1 + \frac{1}{r}\right)\eta_0. \tag{8}$$

We may infer from (5) and (8) that the effective barotropic indexes depend only on the ratio between the energy densities.

Let us now analyze the evolution equation for the ratio between the energy densities, which is given by

$$\dot{r} = -3Hr\mathcal{F}(r), \tag{9}$$

where $\mathcal{F}(r)$ denotes the expression

$$\mathcal{F}(r) = \left[\gamma_{\rm m} - \gamma_{\rm de} + \left(1 + \frac{1}{r}\right)\left(F(r) - \sqrt{3}\eta_0\right)\right]. \tag{10}$$

If we assume a stationary state of the Universe to be attained by a constant value of $r = r_s$, the constant solutions can be found from

$$\left(\frac{{\rm d}\mathcal{F}(r)}{{\rm d}r}\right)_{r=rs} \geq 0, \tag{11}$$

so that we obtain from (10) the inequality

$$r_s\,(1 + r_s)\left(\frac{{\rm d}F(r)}{{\rm d}r}\right)_{r=rs} - \left(F(r_s) - \sqrt{3}\eta_0\right) \geq 0, \tag{12}$$

by taking into account that the barotropic indexes $\gamma_{\rm m}$ and $\gamma_{\rm de}$ are constants. Inspection of (12) shows that the simplest choice, $F = \sqrt{3}\eta_0$, satifies the above inequality. Moreover, the interaction term in the form $3H\lambda\rho_{\rm de}$, with λ a constant and proportional to $\rho_{\rm de}$, is consistent with the Le Châtelier–Braun principle of thermodynamics, as shown by [43].

In order to solve the field equations, we start out by analyzing the evolution equation for the energy density associated with the dark energy (3b). According to the ansatz (5) and our choice for F, the effective barotropic index $\gamma^e_{\rm de} = \gamma_{\rm de} - \sqrt{3}\eta_0$ is a constant. We may hence integrate (3b) to obtain the equality

$$\rho_{\rm de} = \rho^0_{\rm de}\left(\frac{a_0}{a}\right)^{3\gamma^e_{\rm de}}, \tag{13}$$

where we associate the index 0 with the present values of the variables.

Differentiation of the Friedmann equation (1) with respect to time yields the relation

$$\dot{H} + \frac{3}{2}(\gamma_{\rm m} - \sqrt{3}\eta_0)H^2 - \frac{1}{2}(\gamma_{\rm m} - \gamma_{\rm de})\rho^0_{\rm de}\left(\frac{a_0}{a}\right)^{3\gamma^e_{\rm de}} = 0, \tag{14}$$

which we integrate to find an explicit expression for H:

$$H^2 = \mathcal{C}\left(\frac{a_0}{a}\right)^{3(\gamma_{\rm m} - \sqrt{3}\eta_0)} + \frac{\rho^0_{\rm de}}{3}\left(\frac{a_0}{a}\right)^{3\gamma^e_{\rm de}}. \tag{15}$$

The constant of integration $\mathcal{C}$ is fixed by the current values of the cosmic scale factor a_0 and Hubble constant H_0, which yield

$$\mathcal{C} = H_0^2 - \frac{\rho^0_{\rm de}}{3}. \tag{16}$$

Equation (15) can hence be rewritten in terms of the red shift $z = (a_0/a - 1)$ as

$$\frac{H^2}{H_0^2} = \Omega^0_{\rm m}\,(1+z)^{3(\gamma_{\rm m} - \sqrt{3}\eta_0)} + \Omega^0_{\rm de}\,(1+z)^{3\gamma^e_{\rm de}}, \tag{17}$$

where $\Omega_i = \rho_i/(\rho_{\rm m} + \rho_{\rm de})$ denote the density parameters.

From $H^2 = (\rho_{\rm m} + \rho_{\rm de})/3$, we can relate the density parameters for the matter and dark energy to the red shift, namely,

$$\Omega_{\rm m}(z) = \frac{\Omega^0_{\rm m}(1+z)^{3(\gamma_{\rm m} - \sqrt{3}\eta_0)}}{\Omega^0_{\rm m}(1+z)^{3(\gamma_{\rm m} - \sqrt{3}\eta_0)} + \Omega^0_{\rm de}(1+z)^{3\gamma^e_{\rm de}}}, \tag{18}$$

$$\Omega_{\rm de}(z) = \frac{\Omega^0_{\rm de}(1+z)^{3\gamma^e_{\rm de}}}{\Omega^0_{\rm m}(1+z)^{3(\gamma_{\rm m} - \sqrt{3}\eta_0)} + \Omega^0_{\rm de}(1+z)^{3\gamma^e_{\rm de}}}. \tag{19}$$

From the equality $r(z) = \Omega_{\rm m}(z)/\Omega_{\rm de}(z)$, we can then express the ratio between the energy densities as a function of the red shift. Equation (17) moreover allows us to express the non-equilibrium pressure, given by $\varpi = -3\sqrt{3}\eta_0 H^2$, as a function of the red shift.

Also important in cosmology is the deceleration parameter $q = 1/2 + 3w_{\rm e}/2$, here expressed in terms of the effective parameter $w_{\rm e} = (p_{\rm m} + p_{\rm de} + \varpi)/(\rho_{\rm m} + \rho_{\rm de})$. From the barotropic equations of state and from the representation of the non-equilibrium pressure, the effective parameter becomes

$$w_{\rm e} = (\gamma_{\rm m} - 1)\Omega_{\rm m}(z) + (\gamma^e_{\rm de} + \sqrt{3}\eta_0 - 1)\Omega_{\rm de}(z) - \sqrt{3}\eta_0. \tag{20}$$

By inspecting the expressions (17)–(20), we can infer the existence of three free parameters in the proposed model, the coefficients γ_m, η_0, and $\gamma^e_{\rm de}$. In Section 3, an analysis is carried out to set cosmological constraints on the free parameters, and the cosmological solutions are discussed.

3 Cosmological Constraints and Cosmological Solutions

The coefficients $\gamma_{\rm m}$, η_0, and $\gamma^e_{\rm de}$ can be found from the observational cosmological constraints, which are based on the data of the Hubble parameter $H(z)$ presented in Table 1 [44], together with the present values $H_0 = 72$ km/s Mpc, $\Omega^0_{\rm m} = 0.30$, and $\Omega^0_{\rm de} = 0.70$ [45]. The set of values in Table 1 was used in [41], and the adopted methodology is explained in the "Appendix."

For the viscous case, we have considered a dust-like matter field ($\gamma_m = 1$) and adjusted the parameters $\gamma^e_{\rm de}$ and η_0. Figure 1 plots the probability ellipsis in the

Table 1 Hubble parameter $H(z)$, from [44]

z	$H(z)$ (km/s Mpc)	1σ uncertainty
0.09	69	±12
0.17	83	±8.3
0.27	70	±14
0.40	87	±17.4
0.88	117	±23.4
1.30	168	±13
1.43	177	±14.2
1.53	140	±14
1.75	202	±40.4

plane $\gamma^e_{\rm de}$ versus η_0, the best-fit value being indicated by the dot, which corresponds to $\gamma^e_{\rm de} = 0.125445$ and $\eta_0 = 0.0140124$ with $\chi^2 = 9.104007$.

In order to interpret the results for the viscous case, we compare it with the non-viscous one, which refers also to a non-interacting model. In this case, the free parameters are $\gamma_{\rm m}$ and $\gamma^e_{\rm de}$, and in Fig. 2, we show the probability ellipsis in the plane $\gamma^e_{\rm de}$ versus $\gamma_{\rm m}$. The best-fit value is indicated by a dot, which corresponds to $\gamma^e_{\rm de} = 0.0259052$ versus $\gamma_{\rm m} = 1.0051$ with $\chi^2 = 9.1407510$.

In Figs. 1 and 2, the points inside the inner ellipses or between them stand for the true values of parameters with 68.3% and 95.4%, corresponding to 1σ and 2σ confidence regions, respectively.

Once the free model parameters are known, one can analyze the cosmological solutions. We start out by investigating the density parameters, which are plotted as functions of the red shift in Fig. 3, the solid and dashed lines corresponding to the viscous and non-viscous cases, respectively. From the figure, one can infer that the energy transfer from the dark energy to the matter field is more pronounced in the non-viscous case, since the growth (decay) of the matter-field (dark-energy) density parameter shown by the dashed line is more pronounced than that depicted by the solid line. This behavior is expected from the evolution equations for the energy densities [(6) and (7)] in the viscous case and also from Fig. 4, which shows the evolution of the ratio of the two energy densities $r = \rho_{\rm m}/\rho_{\rm de}$ with the red shift. Figure 4 also shows that in the future—i.e., for negative red shifts—there is no difference between the two cases, since both tend to small values. This points to future predominance of the dark energy.

In Fig. 5, the deceleration parameter is plotted for the two cases. The present values of the deceleration parameter $q(0)$ and the value for the red shift z_t at which the transition from a decelerated to an acceler-

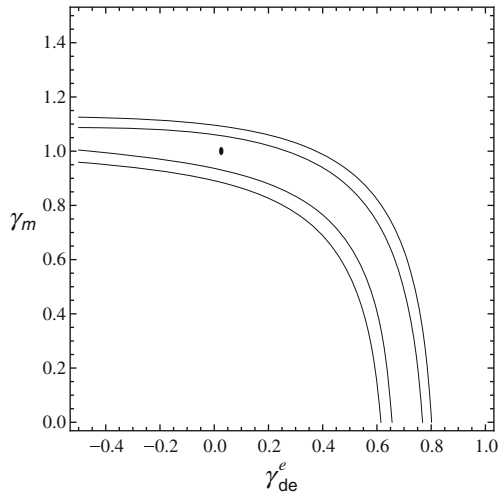

Fig. 2 Confidence regions for the best-fit values for the non-viscous case

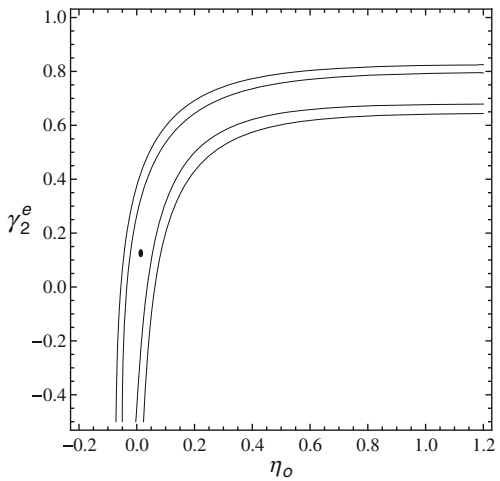

Fig. 1 Confidence regions for the best-fit values for the viscous case

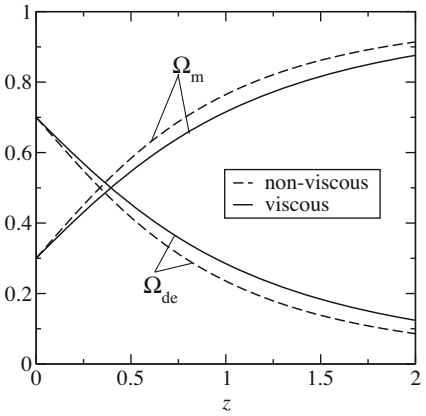

Fig. 3 Density parameters as functions of the red shift z. *Solid lines* viscous; *dashed lines* non-viscous

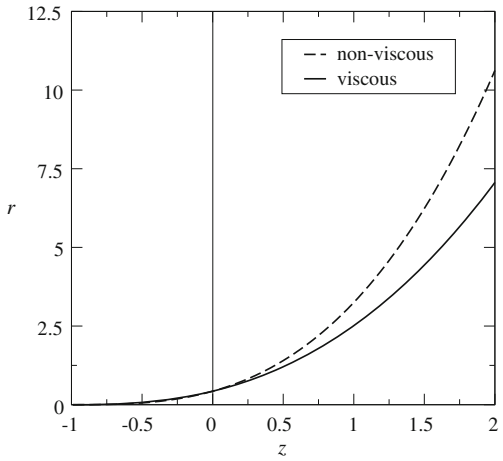

Fig. 4 Ratio between dark matter and dark energy as function of the red shift z. *Solid lines* viscous; *dashed lines* non-viscous

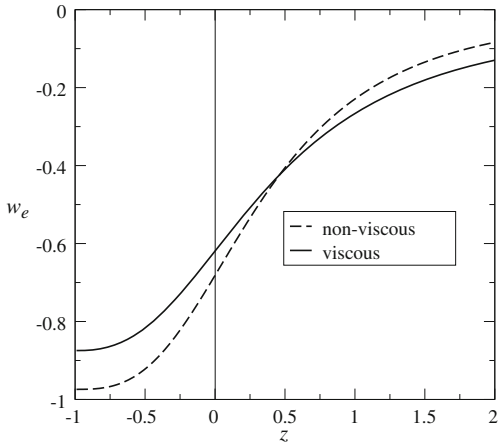

Fig. 6 Effective index w_e as function of the red shift z. *Solid lines* viscous; *dashed lines* non-viscous

ated regime occurs are $q(0) \approx -0.43$ and $z_t \approx 0.74$ for the viscous case and $q(0) \approx -0.52$ and $z_t \approx 0.67$ for the non-viscous case. These values and those in the literature, $q(0) = -0.46 \pm 0.13$ [46] and $z_t = 0.74 \pm 0.18$ [47], are of the same order of magnitude. From the comparison between the viscous and non-viscous cases in this figure, we may infer that in the former the past deceleration is smaller, the transition from a decelerated to an accelerated regime occurs earlier, and the present and future accelerations are smaller.

The effective index w_e is shown in Fig. 6 as a function of the red shift for the viscous and non-viscous cases. We may conclude that in the future, the mixture of matter and dark energy behaves like a quintessence, and the non-viscous case approximates to a cosmological constant with $w_e \approx -1$. For large red shifts, w_e tends to zero and to a small negative value in the non-viscous and viscous cases, respectively. Notice should be taken that large red shifts call for inclusion of a radiation field, which will lead to positive effective indexes.

Figure 7 shows the distance modulus μ_0, the difference between the apparent (m), and the absolute (M) magnitudes of a source, given by the expression

$$\mu_0 = m - M = 5 \log \left\{ (1+z) \int_0^z \frac{\mathrm{d}z'}{H(z')} \right\} + 25, \qquad (21)$$

where the quantity within braces represents the luminosity distance in megaparsecs. The circles in the figure are observational data for supernovae of type Ia, from [48], which presents four different data sets, associated with various light-curve fitters. For practical purposes, we adopted the SALT data set ($R_V = 3.1$). It is possible to conclude that the curve fits well the obser-

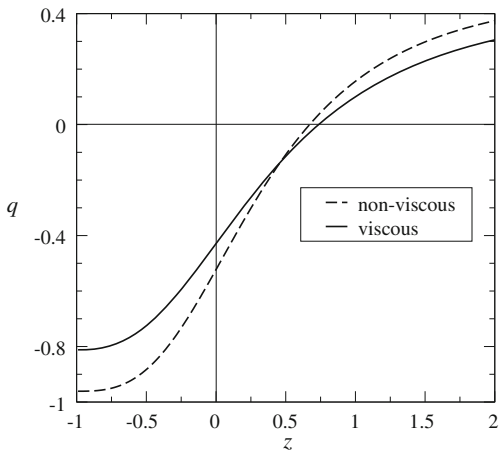

Fig. 5 Deceleration parameter as function of the red shift z. *Solid lines* viscous; *dashed lines* non-viscous

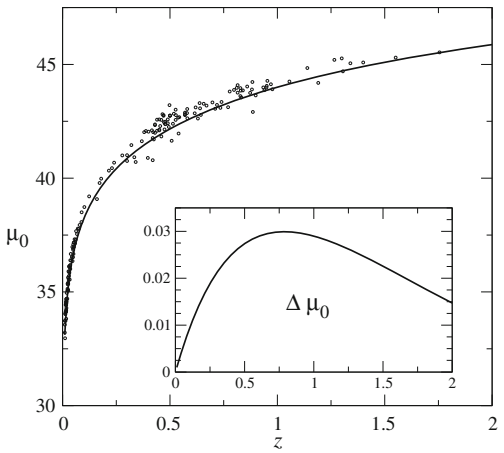

Fig. 7 Distance modulus μ_0 as function of the red shift z. The *inset* shows the difference between the moduli for viscous and non-viscous cases: $\Delta\mu_0 = \mu_0^{\text{viscous}} - \mu_0^{\text{non-viscous}}$

vational data. Moreover, the inset shows no significant difference between the curves for the viscous and non-viscous cases.

4 Conclusions

In this work, we studied a cosmological model with interacting dark fluids in a dissipative Universe where the non-equilibrium pressure is responsible for the irreversible processes. The non-equilibrium pressure was assumed to be proportional to the Hubble parameter within the framework of a first-order thermodynamic theory. Matter and dark energy were coupled through their barotropic indexes, which are functions of the ratio between their energy densities. The function of the ratio between the energy densities—which accounts for the energy transfer between matter and dark energy—follows from the analysis of the differential equation for the density ratio. The observational data of the Hubble parameter were used to set constraints on the free parameters of the model. It was shown that the energy transfer from the dark energy to the matter field is more efficient in the non-viscous case. Furthermore, for both the viscous and non-viscous cases, we concluded that the dark energy density predominates in the future and that the mixture behaves like a quintessence in the future and found deceleration parameters comparable to those in the literature. It was also shown that the predicted behavior of the distance modulus μ_0, which is related to the luminosity distance, fits well the observational values.

Acknowledgements GMK acknowledges fruitful discussions with Luis P. Chimento and Mónica Forte and the support by the CNPq. OASS acknowledges support by the CAPES.

Appendix: Bayesian Inference

In a statistical sense, a physical model may be thought of as described by a set of parameters. These parameters may be determined in many ways; most commonly, one resorts to Bayesian inference, a well-established statistical inference procedure, which estimates model parameters on the basis of evidence. The main purpose of this section is to present a brief introduction to the subject.

For a given model and data set, Bayesian inference employs a probability distribution called *posterior* probability to summarize all uncertainty. This probability distribution is proportional to a *prior* probability distribution (or simply the prior) and a likelihood function. The later, denoted by $\mathcal{P}(\mathbf{D}|\theta)$, is usually defined as the unnormalized probability density of measuring the data $\mathbf{D} = \{D_1, D_2, ..., D_n\}$ for a given model $\mathcal{M}$ in terms of its parameters $\theta = \{\theta_\mathbf{1}, \theta_\mathbf{2}, ..., \theta_\mathbf{n}\}$. For our purposes, it suffices to assume that the measured values are normally distributed around their true value, so that

$$\mathcal{P}(\mathbf{D}|\theta) \propto \exp\left[-\chi^2(\theta)/2\right]. \tag{22}$$

The posterior $\mathcal{P}(\theta|\mathbf{D})$ is determined by Bayes' theorem:

$$\mathcal{P}(\theta|\mathbf{D}) = \frac{\mathcal{P}(\mathbf{D}|\theta)\mathcal{P}(\theta)}{\int \mathrm{d}\theta \mathcal{P}(\mathbf{D}|\theta)\mathcal{P}(\theta)}, \tag{23}$$

where $\mathcal{P}(\theta)$ denotes the prior probability distribution. The prior carries all previous knowledge of the parameters before the measurements were made.

Bayesian inference estimates parameters by maximizing the posterior $\mathcal{P}(\theta|\mathbf{D})$. This is in contrast with the frequentist approach, which maximizes the likelihood $\mathcal{P}(\mathbf{D}|\theta)$. Nevertheless, whenever the so-called uninformative priors are considered, both frameworks lead to the same conclusions. If the measured data are independent from each other as well as Gaussian distributed around their true value, $\mathbf{D}(\theta)$, then maximizing the likelihood $\mathcal{P}(\mathbf{D}|\theta)$ is equivalent to minimizing the chi-square function

$$\chi^2(\theta) \equiv \left(\mathbf{D}^{\mathrm{obs}} - \mathbf{D}(\theta)\right) C^{-1} \left(\mathbf{D}^{\mathrm{obs}} - \mathbf{D}(\theta)\right)^T, \tag{24}$$

where C is the covariance matrix given by the experimental errors. For uncorrelated data, $C_{ij} = \delta_{ij}\sigma_i^2$ and

$$\chi^2(\theta) \equiv \sum_{i=1}^{n} \left(\frac{D^{\mathrm{obs}} - D(\theta)}{\sigma_i^2}\right)^2, \tag{25}$$

where σ_i denotes the experimental errors.

In Bayesian inference, confidence intervals are drawn around the maximal likelihood point, which yields the best fit parameters. It is conventionally used 1σ and 2σ confidence regions with 68.3% and 95.4% probability, respectively, for the true value of parameters. These regions are mathematically defined by the inequalities

$$\chi^2(\theta) - \chi^2(\theta_{\mathrm{bf}}) \leq 2.3, \tag{26}$$

for the 1σ range and

$$\chi^2(\theta) - \chi^2(\theta_{\mathrm{bf}}) \leq 6.17, \tag{27}$$

for the 2σ range, where θ_{bf} denotes the best-fit value of parameters.

References

1. S. Perlmutter, et al., Astrophys. J. **517**, 565 (1999)
2. A.G. Riess, et al., Astrophys. J. **560**, 49 (2001)
3. M.S. Turner, A.G. Riess, Astrophys. J. **569**, 18 (2002)
4. J. Tonry, et al., Astrophys. J. **594**, 1 (2003)
5. M. Persic, P. Salucci, F. Stel, Mon. Not. Roy. Astron. Soc. **281**, 27 (1996)
6. P.J.E. Peebles, B. Ratra, Rev. Mod. Phys. **75**, 559 (2003)
7. V. Sahni, A.A. Starobinsky, Int. J. Mod. Phys. D **9**, 373 (2000)
8. V. Sahni, in *The Physics of the Early Universe*, vol. 653. ed. by E. Papantonopoulos, Lect. Notes Phys. (Springer, Berlin, 2005)
9. S.M. Carroll, Living Rev. Rel. **4**, 1 (2001)
10. T. Padmanabhan, Phys. Rep. **380**, 235 (2003)
11. E.J. Copeland, M. Sami, S. Tsujikawa, Int. J. Mod. Phys. D **15**, 1753 (2006)
12. S. Weinberg, Rev. Mod. Phys. **61**, 1 (1989)
13. P.J. Steinhardt, in *Critical Problems in Physics*, ed. by V.L. Fitch, D.R. Marlow, M.A.E. Dementi (Princeton University Press, Princeton, 1997)
14. L.P. Chimento, A.S. Jakubi, D. Pavon, Phys. Rev. D **62**, 063508 (2000)
15. L.P. Chimento, A.S. Jakubi, D. Pavon, W. Zimdahl, Phys. Rev. D **67**, 083513 (2003)
16. J.B. Binder, G.M. Kremer, Gen. Rel. Grav. **38**, 857 (2006)
17. J.B. Binder, G.M. Kremer, Braz. J. Phys. **35**, 1038 (2005)
18. G.M. Kremer, Gen. Rel. Grav. **39**, 965–972 (2007)
19. G. Huey, B.D. Wandelt, Phys. Rev. D **74**, 023519 (2006)
20. L.P. Chimento, M. Forte, Phys. Lett. B **666**, 205 (2008)
21. R.G. Cai, A. Wang, JCAP **0503**, 002 (2005)
22. Hao Wei, JCAP, **1008**, 20 (2010)
23. L. Amendola, Phys. Rev. D **62**, 043511 (2000)
24. L. Amendola, D. Tocchini-Valentini, Phys. Rev. D **64**, 043509 (2001)
25. L. Amendola, D. Tocchini-Valentini, Phys. Rev. D **66**, 043528 (2002)
26. L. Amendola, C. Quercellini, D. Tocchini-Valentini, A. Pasqui, Astrophys. J. **583**, L53 (2003)
27. W. Zimdahl, D. Pavon, Phys. Lett. B **521**, 133 (2001)
28. D. Pavon, B. Wang, Gen. Rel. Grav. **41**, 1 (2009)
29. L.P. Chimento, Phys. Rev. D **81**, 043525 (2010)
30. G.L. Murphy, Phys. Rev. D. **8**, 4231 (1973)
31. Ø. Grøn, Astrophys. Space Sci. **173**, 191 (1990)
32. G.M. Kremer, F.P. Devecchi, Phys. Rev. D **65**, 083515 (2002)
33. V.A. Belinskiĭ, E.S. Nikomarov, I.M. Khalatnikov, Sov. Phys. JETP **50**, 213 (1979)
34. V. Romano, D. Pavón, Phys. Rev. D **47**, 1396 (1993)
35. L.P. Chimento, A.S. Jakubi, Class. Quant. Grav. **10**, 2047 (1993)
36. A.A. Coley, R. J. van den Hoogen, Class. Quant. Grav. **12**, 1977 (1995)
37. W. Zimdahl, Phys. Rev. D **61**, 083511 (2000)
38. G.M. Kremer, Gen. Relat. Grav. **35**, 1459 (2003)
39. G.M. Kremer, Phys. Rev. D **68**, 123507 (2003)
40. G.M. Kremer, M.C.N. Teixeira da Silva, Braz. J. Phys. **34** 1204 (2004)
41. L.P. Chimento, M. Forte, G.M. Kremer, Gen. Rel. Grav. **41**, 1125 (2009)
42. C. Cercignani, G.M. Kremer, *The Relativistic Boltzmann Equation: Theory and Applications*, (Birkhäuser, Basel, 2002)
43. D. Pavón, B. Wang, Gen. Relativ. Grav. **41**, 1 (2009)
44. C. Ma, T.-J. Zhang, Astrophys. J. **730**, 74 (2011)
45. W.L. Freedman, et al., Astrophys. J. **553**, 47 (2001)
46. J.M. Virey, et al., Phys. Rev. D **72**, 061302 (2005)
47. A.G. Riess, et al., Astrophys. J. **607**, 665 (2004)
48. M. Hicken, et al., Astrophys. J. **700**, 1097–1140 (2009)
49. G.M. Kremer, F.P. Devecchi, Phys. Rev. D **66**, 063503 (2002)
50. G.M. Kremer, F.P. Devecchi, Phys. Rev. D **67**, 047301 (2003)